Poormohammad *et al.*
J Wireless Com Network (2022) 2022:88
https://doi.org/10.1186/s13638-022-02177-5

EURASIP Journal on Wireless Communications and Networking

RESEARCH Open Access

The effect of far-field cylindrical scatterers on radio direction finding and beamforming estimated by cylindrical array of dipoles

Sarah Poormohammad[1*], Forouhar Farzaneh[2] and Ali Banai[2]

*Correspondence:
s.poormohammad@urmia.ac.ir

[1] Department of Electrical and Computer Engineering, Urmia University, Urmia, Urmia 5756151818, Iran
[2] Department of Electrical Engineering, Sharif University of Technology, Tehran, Tehran 11155-4363, Iran

Abstract

Direction finding using a cylindrical array of dipoles has been implemented in presence of large cylindrical scatterers. A different number of scatterers in the simulations are used. The effect of the large cylindrical scatterers is considered by cylindrical harmonic expansion of the scattered field. These fields are computed analytically. The direction finding process is verified by a comparison with phase difference direction finding method implemented in HFSS simulator environment. The error induced in the direction finding mechanism by the scattered fields is estimated through Monte-Carlo simulations. Interfering signals are introduced and a beamforming process is implemented to evaluate the corresponding signal to interference ratios. The method alleviates the use of high computational cost simulations for scatterer effect estimation. The method could be used in wireless communication and smart antenna applications.

Keywords: Scattering, Far-field, Direction finding, MUSIC algorithm, Beamforming, Mutual coupling, 3D dipole array, Monte-Carlo simulation

1 Introduction

The smart antennas are widely established in different wireless systems to enhance the spectrum efficiency by increasing the signal to noise ratio. The interest in smart antennas for airplane and aerospace applications such as localization, tracking, navigation and surveillance systems is growing increasingly [1]. For this purpose, the radio direction finding and the beamforming methods were studied to improve the capabilities of antenna arrays in different airplane and airport services [2–4]. In a more realistic situation such as airports, the effects of the scatterer in the presence of the mutual coupling between the antenna elements are not negligible and it should be considered in the corresponding models [5]. A maximum likelihood DOA (direction of arrival) estimator was established in the presence of a local scatterer without considering the mutual coupling effects in [6]. The studies in [7] and [8] proposed an iterative algorithms based on the self-calibration methods for direction finding to remove the effects of the mutual coupling and the 3D scatterer. These iterative methods had a limited application where the time delay/computation time

is important. As the electrical size or the number of scatterers is increased, the efficiency of the algorithms in [7] and [8] is decreased. The issue of the far-field large scatterer has not been addressed in [7] or [8]. In [8] the authors established a calibration method to mitigate the multipath signal components in presence of scatterer for direction finding and localization. The method in [8] was a time-consuming method due to its numerical electromagnetic tools, especially when the number of scatterers was increased. In addition, the authors in [9] simulated the problem to localize its near-field multi-paths without any far-field scattering components. The effects of large far-field scatterer in DOA estimation for antenna arrays have not been studied as well.

The effects of the coherent local scattering in adaptive beamforming were considered as a mismatch in construction of the IPN (interference-plus-noise) covariance matrix in [10]. The proposed IPN covariance matrix in the algorithm of [10] consisted of the two parts. The first part was obtained by Capon spectrum estimator integrated over a region separated from the direction of the desired signal and the second part was acquired by removing the desired signal component from the sample covariance matrix [10]. The approach to combine the two parts to obtain a good performance in different situations is also an open topic for the researchers. In [11] the authors conducted a cost-effective low rank algorithm for designing a robust adaptive beamforming and the presence of local scatterer was modeled by steering vector mismatches.

The effect of a cylindrical reflector/scatterer at the proximity of three-dimensional cylindrical array was formulated for direction finding and beamforming algorithms in the presence of mutual coupling effects [12].

In this paper, the effect of large far-field scatterers at the proximity of the antenna array in presence of mutual coupling is presented. In this model the scattered field is analytically formulated in terms of the cylindrical harmonics and then the total field is computed for direction finding and beamforming purpose. In an earlier study, the scatterer problem was approximated as a cylinder and the cylindrical harmonic expansion was used for modeling the scattered signal [7]. As mentioned above the algorithm in [7] was iterative and did not guarantee the convergence. It also required a large number of antennas and examined only for near-field scatterers.

In this paper, a number of large cylindrical scatterers are considered and using an array with a limited number of elements the problem of direction finding and beamforming is addressed using the standard MUSIC algorithm in presence of mutual coupling. Finally, the direction finding error and the signal to interference ratio is estimated.

In the following section, we present the algorithms of direction finding and beamforming in presence of large cylindrical scatterers and we compare the direction finding results with the HFSS (high frequency simulation software) simulations. For this purpose, we have implemented a direction finding process using two orthogonal dipole arrays within the HFSS simulator. In Sect. 3 the RMSE (root-mean-square error) values of the direction finding and the SIR (signal to interference ratio) values of the beamforming in the presence of the scatterers and mutual coupling effects are computed for a 3D geometry. Section 4 draws the conclusion.

2 Methods to implement the direction finding and the beamforming algorithms in presence of large cylindrical scatterers

In this section, we first consider the model for scattering of a plane wave by a number of parallel large circular cylinders. Each cylinder is defined by its radius and axis coordinate $(\rho_i^{'}, \varphi_i^{'})$ with respect to the global cylindrical system (ρ, φ) as shown in Fig. 1. Let consider a number of M cylindrical scatterers [13] and the receiving array is considered at the origin of the coordinates.

Considering the TMz incident field (TMz stands for transverse magnetic with respect to the propagation direction z), the incident electric field of a plane wave on the cylinder "i" is expressed as an expansion of Bessel functions in the (ρ_i, φ_i) cylindrical coordinate system as [13]:

$$E_z^{inc}(\rho_i, \varphi_i) = E_0 e^{jk_0\rho_i^{'}\cos\left(\varphi_i^{'}-\varphi_0\right)} e^{jk_0\rho_i\cos(\varphi_i-\varphi_0)} = E_0 e^{jk_0\rho_i^{'}\cos\left(\varphi_i^{'}-\varphi_0\right)} \sum_{n=-\infty}^{n=+\infty} j^{-n} J_n(k_0\rho_i) e^{jn(\varphi_i-\varphi_0)} \tag{1}$$

where k_0 is the free space wave number and φ_0 is the angle of incidence of the plane wave. The expression of the scattered field for perfectly conducting cylinder "i" is given by [13, 14].

$$E_{z,i}^{s}(\rho_i, \varphi_i) = E_0 e^{jk_0\rho_i^{'}\cos\left(\varphi_i^{'}-\varphi_0\right)} \times \sum_{n=-\infty}^{n=+\infty} \frac{(-j)^{-n} J_n(k_0 a)}{H_n^2(k_0 a)} H_n^2(k_0\rho_i) e^{jn(\varphi_i-\varphi_0)} \tag{2}$$

where a is the radius of a large cylindrical scatterer in the far-field of the antenna array and it is considered to be small with respect to the wavelength.$H_n^2(k_0\rho_i)$ is Hankel function of the second kind. After computing the scattered field by each of the cylinders one can replace the local coordinate (ρ_i, φ_i) by global coordinate (ρ, φ) using the following equations,

$$x = \rho\cos(\varphi) - \rho_i^{'}\cos\left(\varphi_i^{'}\right)$$

$$y = \rho\sin(\varphi) - \rho_i^{'}\sin\left(\varphi_i^{'}\right)$$

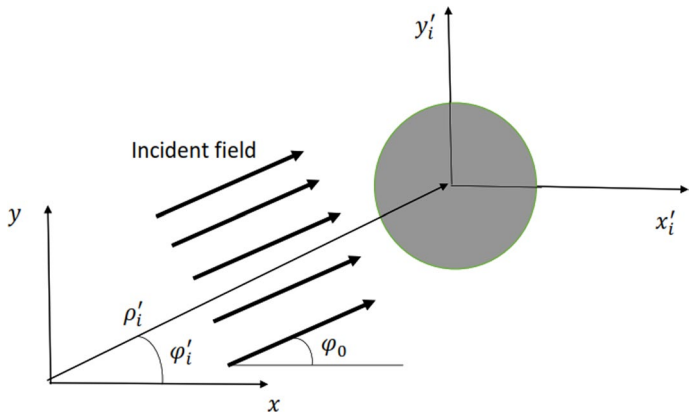

Fig. 1 The cross section of circular cylinder "i" upon which the plane wave is incident

$$\rho_i = \sqrt{x^2 + y^2}$$

$$\varphi_i = \tan^{-1}\frac{y}{x} \tag{3}$$

Considering M scatterers, at any point the total electric field is

$$E_z(\rho,\varphi) = E_z^{inc}(\rho,\varphi) + \sum_{i=1}^{M} E_{z,i}^{s}(\rho,\varphi) \tag{4}$$

Now, for considering the effect of scatterers in direction finding and beamforming processes we should use Eq. (4) for the total incident field on the antenna array.

2.1 Direction finding in presence of large cylindrical scatterers

For direction finding purpose a cylindrical array of 6 half-wave dipole antennas is considered in presence of a few large cylindrical scatterers in the far-field region. The distance between the antenna elements is $\frac{\lambda}{2}$ and thus the radius of the cylindrical array (r_c) is $\frac{\lambda}{2}$ according to (5). This formula is calculated by trigonometric relationships for the proposed geometry.

$$r_c = \frac{\lambda/2}{2sin(\pi/6)} \tag{5}$$

As we desire to have the scatterers in the far-field of the array and the scatterers to be adequately large, here the distance between the cylindrical scatterer and the center of the cylindrical array is considered to be 10λ and the height of the cylindrical scatterer is considered to be 10λ. The geometry of the cylindrical array including one cylindrical scatterer is shown in Fig. 2.

The search function (pseudospectrum) of the modified MUSIC method (to perform the direction finding algorithm) as a function of the array steering vector $\boldsymbol{a}(\theta,\varphi)$ can be expressed as (6), to include the mutual coupling effect [15].

$$\boldsymbol{P}_{MUSIC}(\theta,\varphi) = \frac{1}{\left|\boldsymbol{a}^H(\theta,\varphi)(\boldsymbol{Z}_0^{-1})^H\boldsymbol{E}_n\boldsymbol{E}_n^H\boldsymbol{Z}_0^{-1}\boldsymbol{a}(\theta,\varphi)\right|} \tag{6}$$

In general, the steering vector $\boldsymbol{a}(\theta,\varphi)$ with wavenumber of k_c is defined as (7), where $\boldsymbol{r_m}$ is the position vector of each array element m and $\boldsymbol{r_i}$ is the unit vector in the direction of the field point [15].

$$\boldsymbol{a}(\theta,\varphi) = e^{-jk_c(\boldsymbol{r_i}.\boldsymbol{r_m})} \tag{7}$$

Here, the direction finding algorithm is performed in presence of the incident field and the scattered field. In order to validate our model including the scatterer effect we compare our results with those in an HFSS simulation environment. For this purpose, we use the geometry of Fig. 2 for direction finding with modified MUSIC algorithm. As an example the azimuth and elevation angles of the incident signal are considered to be

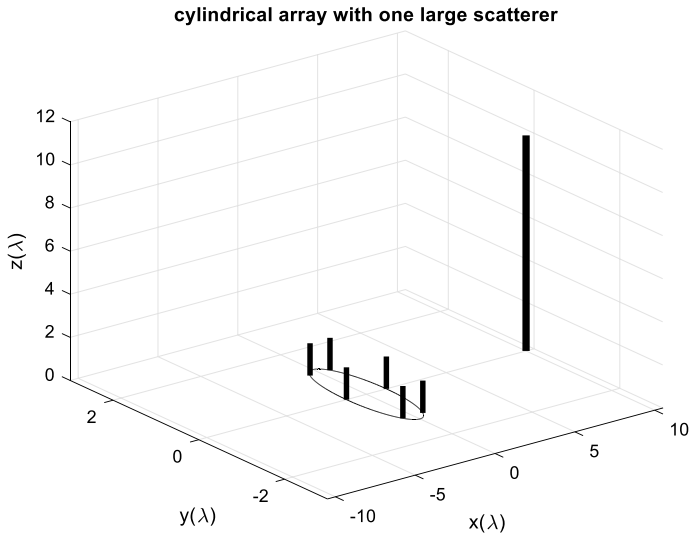

Fig. 2 The geometry of the cylindrical array with a single cylindrical scatterer in this work

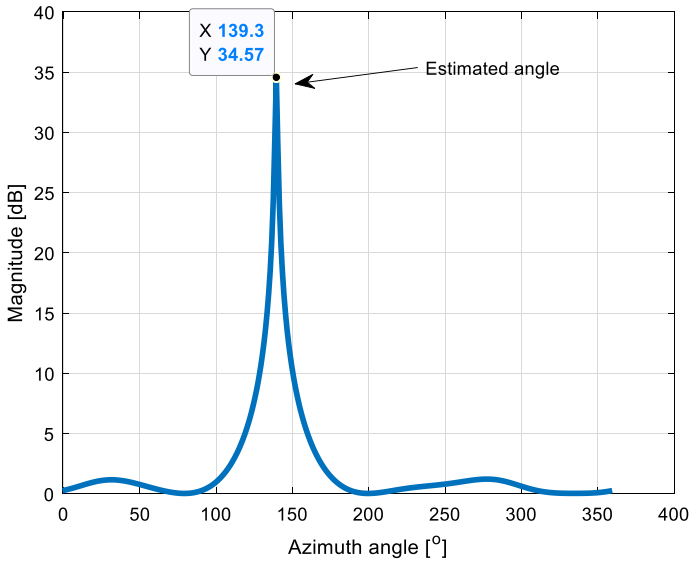

Fig. 3 The magnitude of pseudospectrum function of MUSIC DOA algorithm as a function of azimuth angle with a single cylindrical scatterer

$\varphi = 140^{\circ}$ in horizontal plane ($\theta = 90^{\circ}$). The number of snapshots is 100 and the value of SNR is 10 dB in the simulation. The modified MUSIC Pseudospectrum as a function of azimuth angle for the defined geometry is shown in Fig. 3.

As shown in Fig. 3 the proposed model estimates the azimuth direction of arrival angle properly in the presence of the far-field cylindrical scatterer. To verify this model, we implement two orthogonal array of dipoles and we estimate the angle of arrival by HFSS simulation, through phase comparison DF (Direction Finding) as described in the following. For this purpose, we consider the geometry of the array with four half-wave dipole antennas in presence of the large far-field scatterer as in

Fig. 4. Here, the center frequency in HFSS simulations is equal to 1 GHz and the elements' distances in each pair (for avoiding phase ambiguity) are considered to be 0.35 λ. The height and the position of the far-field scatterer are the same as before.

To estimate the direction of arrival (by phase comparison DF method) using the geometry of Fig. 4 we first calculate the phase difference of the received signal for each dipole pair in the horizontal lane ($\theta = 90^{\circ}$). For this array the phase difference between the received signal of the elements $\Delta\varphi_{13}$ and $\Delta\varphi_{24}$ is given by (8) and (9),

$$\Delta\varphi_{13} = \varphi_1 - \varphi_3 = kd_s cos(\varphi_0) \tag{8}$$

$$\Delta\varphi_{24} = \varphi_2 - \varphi_4 = kd_s sin(\varphi_0) \tag{9}$$

where k is the wave-number of the incident signal, d_s is the dipoles baseline distance and the φ_0 is the estimated azimuth angle. Using HFSS simulation results in Eqs. (8) and (9), the azimuth angle of arrival is estimated about $\varphi_0 = 137.12^{\circ}$ where the incident angle was at $\varphi = 140^{\circ}$.

To certify more our verifications we consider a number of incident angles $\varphi_0 \in (0, \pi)$ for direction finding with proposed method compared to the phase difference method (implemented by HFSS). The estimated angle in each case was computed through both methods and the results of the estimated angles are depicted in Fig. 5.

The simulations show that the proposed method follows the HFSS simulations quite adequately. Now, we consider a scenario with 3 far-field cylindrical scatterers as in Fig. 6 and compare the angle of arrivals estimated by the proposed method with those of the phase difference method for a number of incident angles. The estimated angles are depicted in Fig. 7.

As a scenario including an interfering signal, we consider the geometry of Fig. 6 for direction finding with the modified MUSIC algorithm including the effects of far-field scatterers for azimuth and elevation angles of the signal and the interference as listed in Table 1.

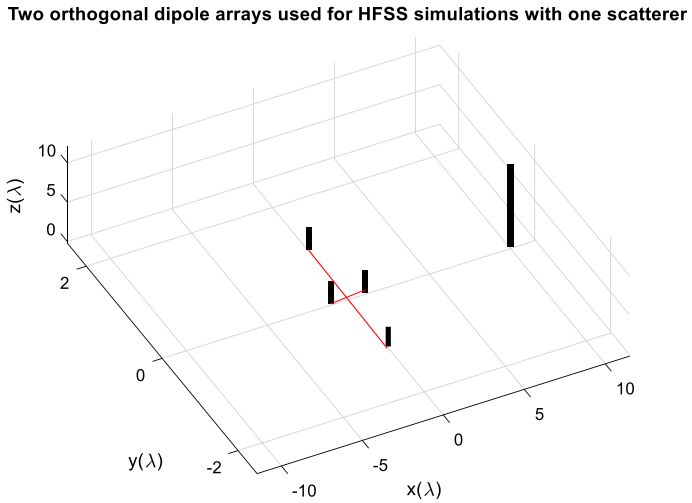

Fig. 4 The geometry of the array with a single cylindrical scatterer and two orthogonal dipole arrays used for HFSS simulations

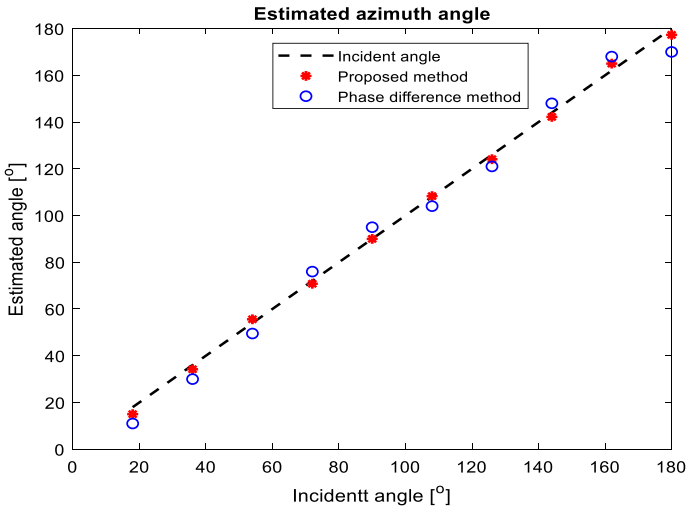

Fig. 5 Estimated angle of arrivals versus the true incident angle with proposed method compared to the phase difference method (implemented by HFSS) with a single scatterer

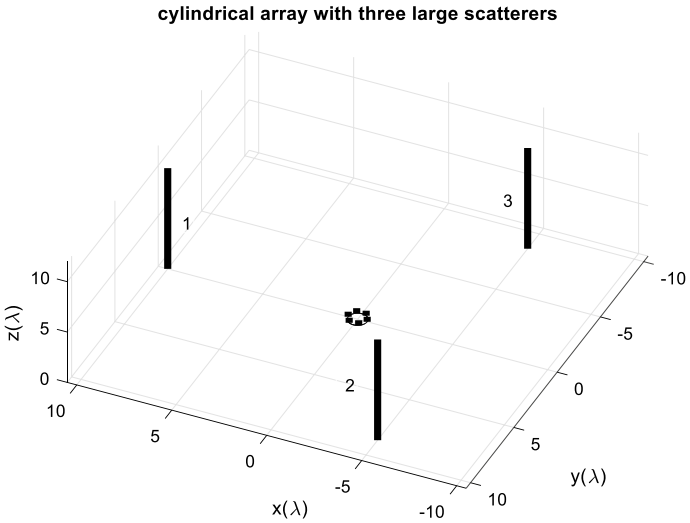

Fig. 6 The geometry of cylindrical array with three cylindrical scatterers

For these simulations the number of snapshot is considered as 100 and the value of the SNR is considered to be 10 dB. The scattered field by three cylindrical scatterers is combined in (4) to achieve the total electric field impinging on the array and the two-dimensional MUSIC Pseudospectrum as a function of azimuth and elevation angles is shown in Fig. 8.

As shown in Fig. 8, the proposed method can determine the angle of arrival for the signal and the interference in presence of the far-field scatterers and mutual coupling effects with minor errors.

2.2 Beamforming in presence of large cylindrical scatterers

In this research, the sub-optimal beamforming method of [16] was modified for considering the effects of scatterers by changing the form of the received signals

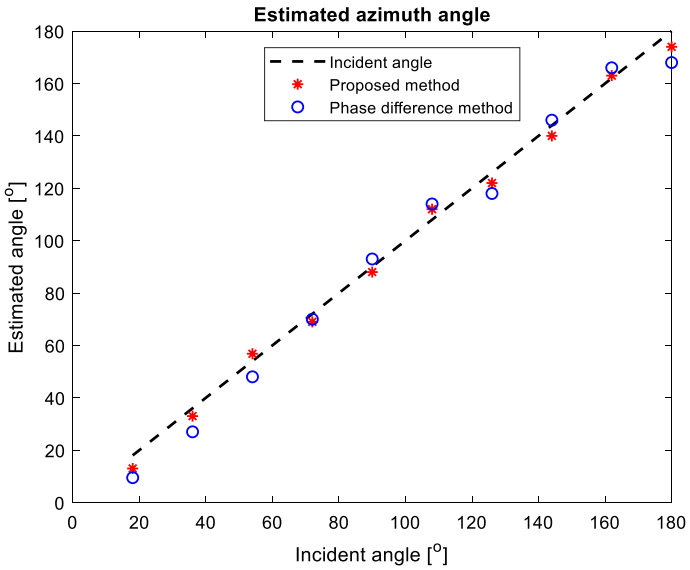

Fig. 7 Estimated angle of arrivals versus the true incident angle with proposed method compared to the phase difference method (implemented by HFSS) with three far-field scatterers

Table 1 The sample azimuth and elevation angles of the signal and the interference for direction finding

Angle	Azimuth	Elevation
Signal	140	65
Interference	50	15

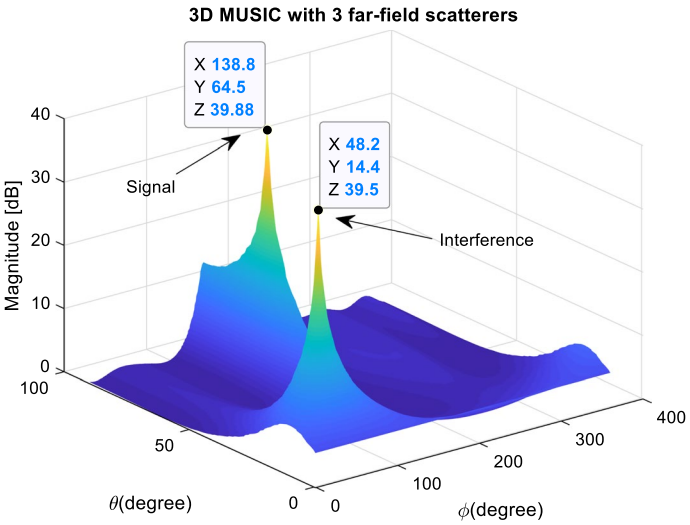

Fig. 8 MUSIC Pseudospectrum function in presence of three far-field scatterers for one incident signal and one interference

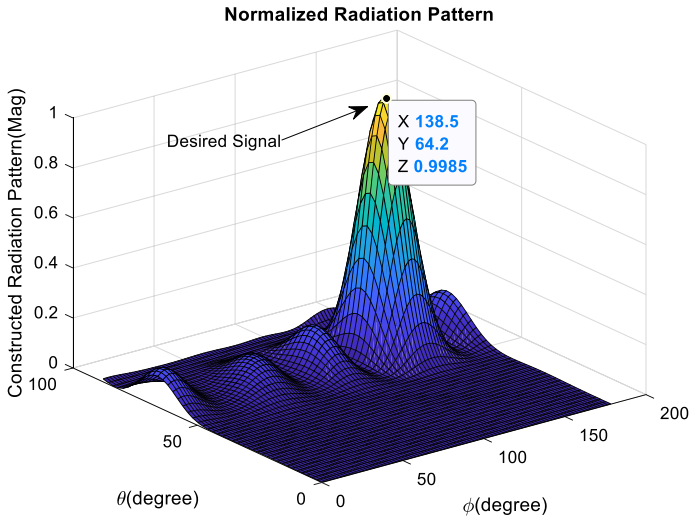

Fig. 9 Normalized radiation pattern of beamforming in presence of three far-field scatterers (linear scale)

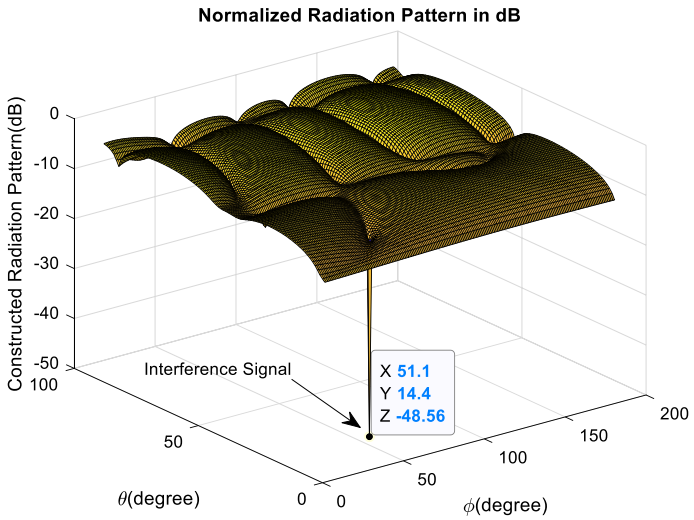

Fig. 10 Normalized radiation pattern of beamforming in presence of three far-field scatterers in dB scale to demonstrate the null depth at the direction of the interference

as described by Eq. (4). The calculations of the optimum weights were conducted through the analytical method based on the active element pattern and the mutual impedance matrix [16]. To evaluate the efficiency of the proposed method in beamforming process, we consider the geometry of dipoles as in Fig. 6 and the scenario of angle of arrivals as in Table 1. After the calculation of the optimum weights, the normalized radiation pattern as a function of the azimuth and elevation angles is depicted in Fig. 9. The radiation pattern, in dB scale, is shown again in Fig. 10 to better demonstrate of the null depth (the direction of interference).

As it is evident in Figs. 9 and 10 the beamforming process has quite satisfactorily optimized the direction of the main beam and the main null.

Instead of a particular scenario, to examine the efficiency of the proposed method in direction finding and beamforming, we have performed a number of Monte-Carlo simulations for different direction of arrivals. The comparison of these Monte-Carlo simulations with and without scatterers is conducted in Sect. 3.

3 Results and discussion: direction finding RMSE and received SIRs estimations

In this section, we compare the two different 3D geometries with and without the scatterers to examine the effects of the scatterers on the RMSE (Root-Mean-Square error) values of the proposed direction finding algorithm. In addition, we consider the two cases with three scatterers and six scatterers and the RMSE values of the arrival angle are computed as follows [15].

$$\mathrm{RMSE} = \frac{1}{2TN}\sum_{n=1}^{T}\sum_{i=1}^{N}\left(\widehat{\theta_i^n} - \theta_i^n\right)^2 + \left(\widehat{\varphi_i^n} - \varphi_i^n\right)^2 \tag{10}$$

where, $\left(\varphi_i^n, \theta_i^n\right)$ are the random angles of incidence signal and interferences and the $\left(\widehat{\varphi_i^n}, \widehat{\theta_i^n}\right)$ are the corresponding estimated angle of arrivals. In (10) T and N are the number of random scenarios and the number of sources. The Monte-Carlo simulations are conducted for 3D array geometry of cylindrical dipoles as in Fig. 11a, b with and without scatterers. We use a cylindrical array including 6 elements in each plane separated by $\frac{\lambda}{2}$ distance. The distance between consecutive planes is λ. The distance between the cylindrical scatterer and the axis of the cylindrical array is considered to be of order of 10λ and the height of the each cylindrical scatterer is quite large (several 10λ's).

To sketch the RMSE values versus the number of snapshots we consider $N=5$ uncorrelated signal sources with 10,000 random scenarios for azimuth and elevation angles with the incidence angles $\theta_i^n \in \left[-\frac{\pi}{2}, \frac{\pi}{2}\right]$ and $\varphi_i^n \in [0, 2\pi]$. The signal to noise ratio is fixed at SNR = 7 dB and the simulations are conducted for the number of snapshots between 20 and 200. These simulations are conducted for different distances $d = 10\lambda$,15λ,20λ, 40λ between the cylindrical scatterers and the axis of the cylindrical array for the cases with three scatterers and six scatterers. The results are shown in Fig. 12a, b.

The comparison of RMSE values with and without the scatterers as a function of the SNR is sketched in Fig. 13a, b at fixed number of snapshots ($L = 100$) for 10,000 random scenarios for azimuth and elevation angles.

As it is shown in Fig. 12 the RMS error is decreased with increasing the number of snapshots while it is increased by reducing the distance of the scatterers. Furthermore, in Fig. 13 it is shown that the RMS error is decreased with increasing the SNR and it is increased by reducing the scatterers distance. The RMS error is increased with increasing the number of large cylindrical scatterers as well. An 80% increase in the RMS Error is observed in Fig. 13b for 6 scatterers at shorter distance.

In this section, we use a modified sub-optimal beamforming method [16] to evaluate the efficiency of the proposed method with three and six far-field scatterers. The beamforming process is conducted using estimated angle of arrivals and the mean values of SIR versus the number of interferences are shown in Fig. 14a, b.

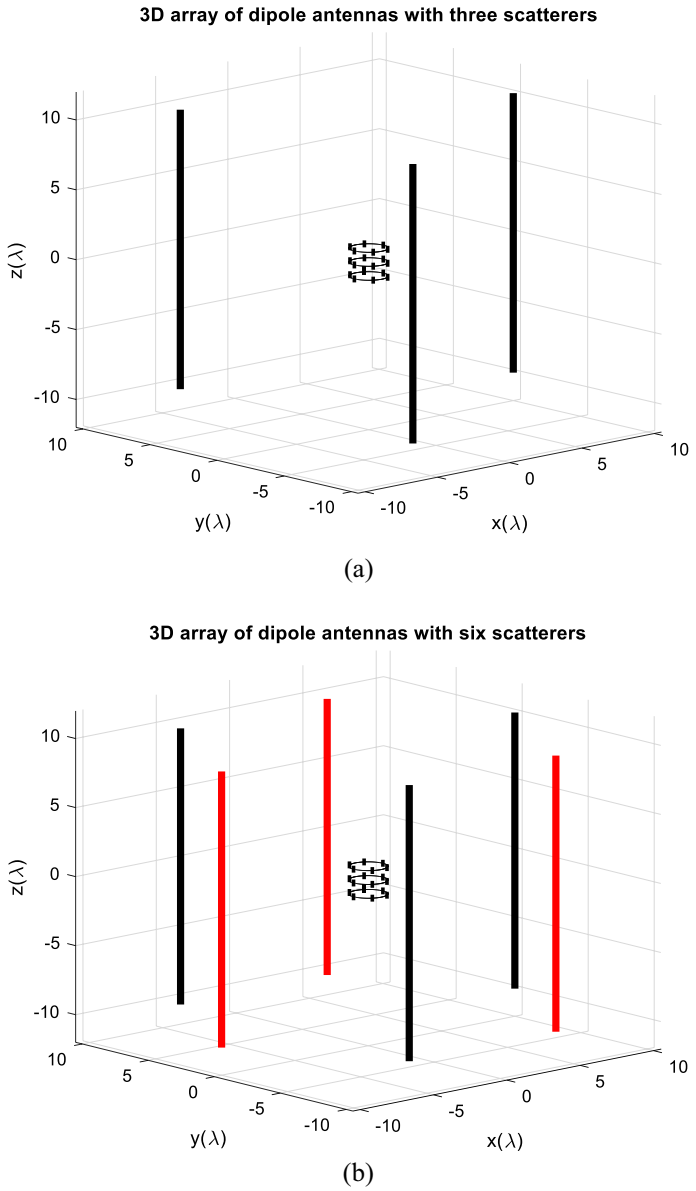

Fig. 11 Three-dimensional cylindrical array of half-wave dipole antennas in presence of **a** three large cylindrical scatterers, **b** six large cylindrical scatterers (three more scatterers are added with red color)

As it is seen in Fig. 14b with three scatterers at a distance of 10λ about 8 dB decrease in SIR is observed compared to no scatterer case while increasing the distances of the scatterers to 40λ about 1.5 dB decrease in the SIR is observed compared to the no scatterer case. In all cases the SIR is monotonically decreased with the number of interferences.

4 Conclusion

In this work, the effect of a limited number of large far-field cylindrical scatterers on the process of direction finding and beamforming by an array of cylindrical dipoles was studied. For verification purpose, we have compared the direction finding results with those of phase comparison method implemented by HFSS in full wave

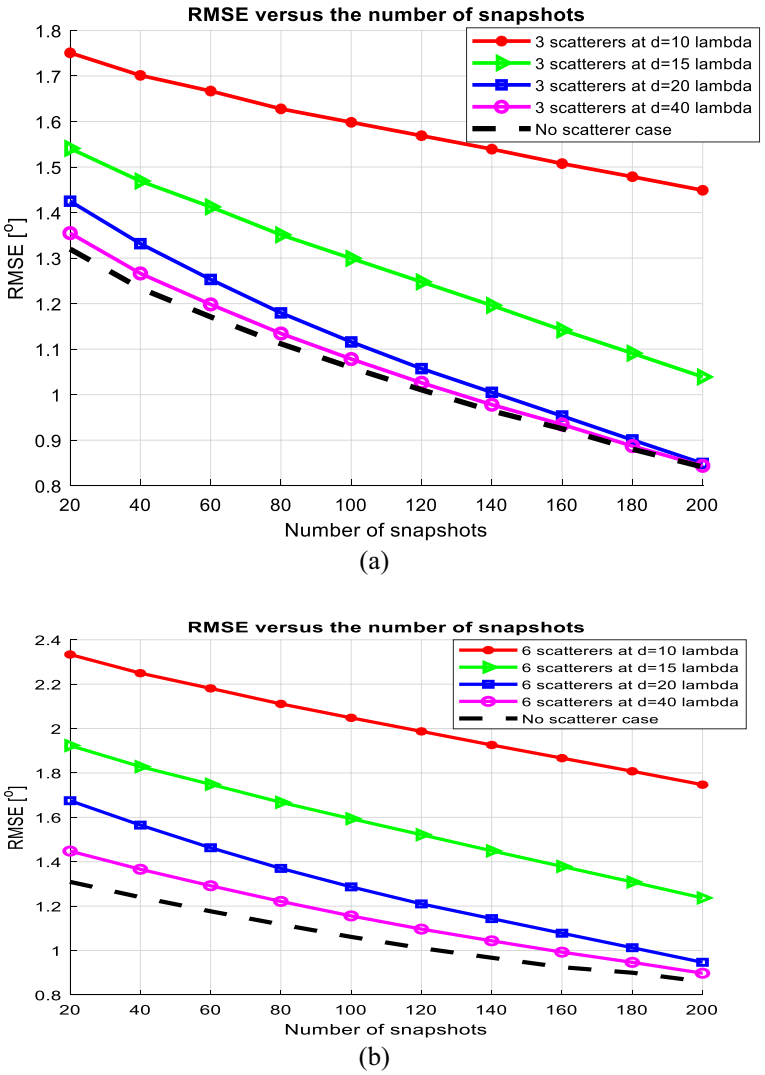

Fig. 12 RMSE values versus the number of snapshots using the geometries of Fig. 11 in presence of scatterers at $d = 10\lambda, 15\lambda, 20\lambda, 40\lambda$ distances compared to no scatterer case, at fixed SNR = 7 dB **a** three large cylindrical scatterers, **b** six large cylindrical scatterers

electromagnetic simulation environment. The comparison results were quite satisfactory. Through our calculations, we have considered the forward scattered fields by the cylindrical scatterers analytically to estimate the angle of arrivals of both the signal and the interferences to perform the beamforming process consequently.

We performed Monte-Carlo simulations to estimate the RMSE values in direction finding and the SIR in beamforming. Here, the computations showed up to 80% increase in RMS Error values in direction finding, and the consequently up to 8 dB's decrease in SIR, depending on the number of scatterers and their distances.

Given the fact that we have used an analytical cylindrical harmonic expansion for the scattered fields, in the problem of direction finding in presence of far-field scatterers, we have greatly reduced the computational cost (compared to the HFSS or other

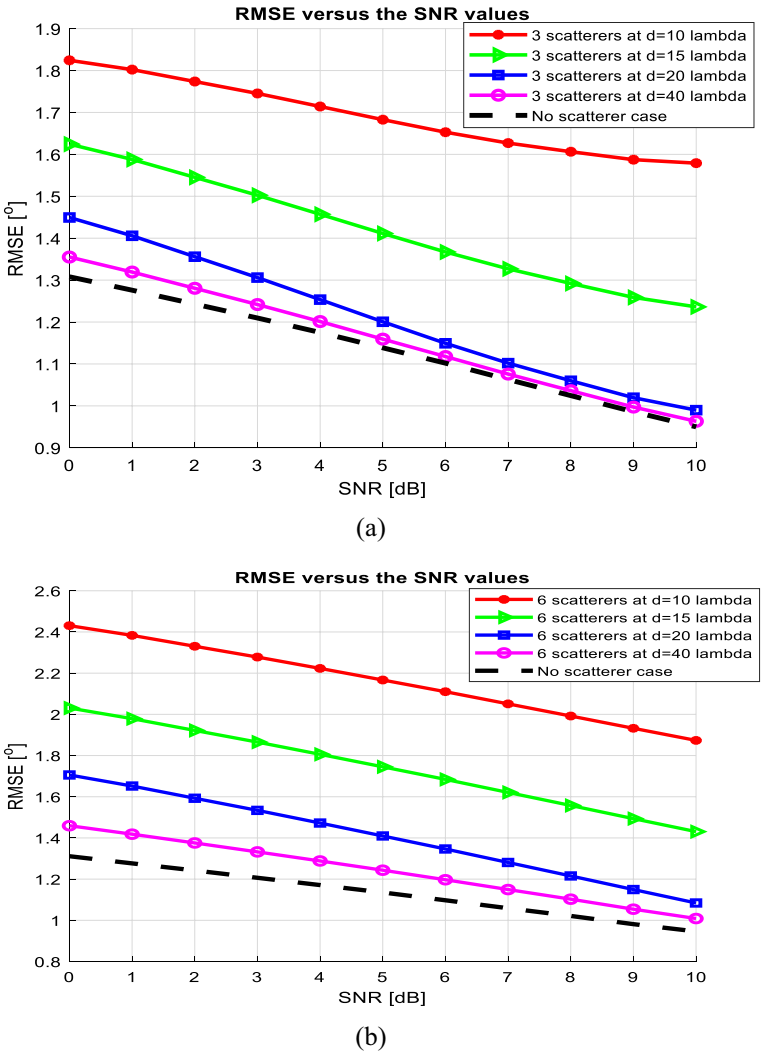

Fig. 13 RMSE values versus the SNR using the geometry of Fig. 11 in presence of far-field scatterers at $d = 10\lambda, 15\lambda, 20\lambda, 40\lambda$ distances compared to no scatterer case, at fixed number of snapshots($L = 100$) **a** three large cylindrical scatterers, **b** six large cylindrical scatterers

full wave numerical electromagnetic simulator). As such, we were able to perform thousands of simulation cases needed in a Monte-Carlo evaluation of errors. By this method, one can increase the number of the scatterers as desired without increasing the computational burden as much. As analytical formulation is used for the scattered fields, it is possible to consider more complex scatterers using several number of conducting cylinders.

Our study showed that the effect of large scatterers can become insignificant for large distances of order of several 10 λ's.

The cylindrical scatterer method could be used in wireless communications, for smart antennas and eventually for the field test of direction finders at the airports or large field test areas.

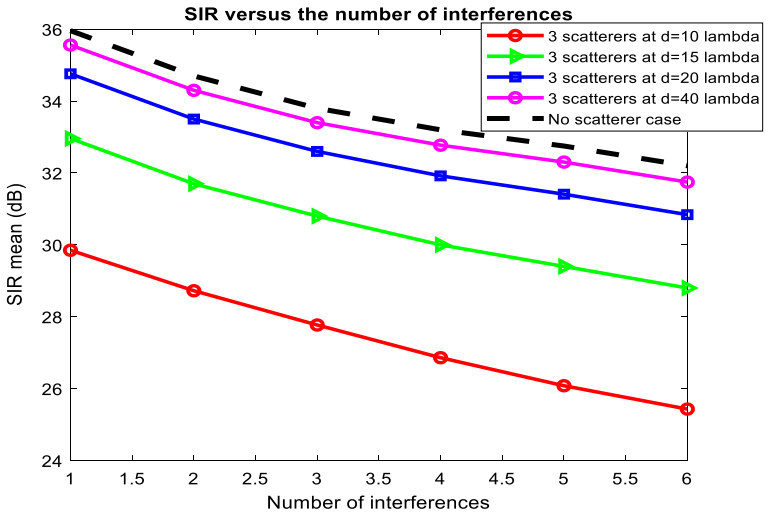

(a)

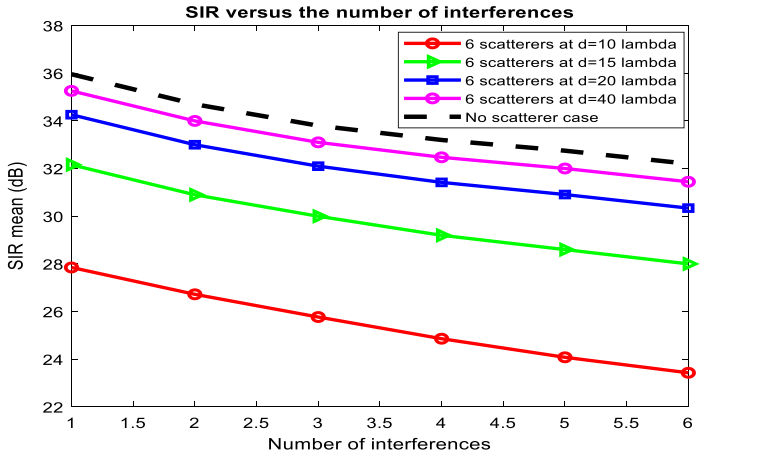

(b)

Fig. 14 Mean values of the SIR versus the number of interferences in presence of the scatterers at $d = 10\lambda, 15\lambda, 20\lambda, 40\lambda$ compared to no scatterer case **a** three large cylindrical scatterers, **b** six large cylindrical scatterers

Abbreviations

SIR	Signal to interference ratio
MUSIC	Multiple signal classification
HFSS	High frequency simulation software
rms	Root-mean-square
RMSE	Root-mean-square error
DOA	Direction of arrival
DF	Direction finding
SNR	Signal to noise ratio
3D	3 Dimensional
IPN	Interference-plus-noise

Acknowledgements
This research was supported by Iran National Science Foundation (INSF).

Author contributions
SP carried out the implementation of the algorithms in MATLAB and HFSS, participated in the alignment and drafted the manuscript. FF participated in the design of the study and helped to draft the manuscript. AB participated in the sequence alignment. All authors read and approved the final manuscript.

Funding
This research has been funded by INSF (Project No: 97019529).

Declarations

Competing interests
The authors declare that they have no competing interests.

Received: 20 April 2022 Accepted: 12 September 2022
Published online: 22 September 2022

References

1. J. Verpoorte, H. Schippers, C.G.H. Roeloffzen, et al., Smart antennas in aerospace applications, in *Paper Presented at 2010 URSI International Symposium on Electromagnetic Theory, Berlin, Germany*, 16–19 August 2010
2. T. Otsuyama, J. Honda, A study of direction finding method for passive airport surveillance radar, in *Paper Presented at 2014 International Symposium on Antennas and Propagation, Kaohsiung, Taiwan*, 2–5 December 2014
3. A. Novak, Radio direction finding in air traffic services. Promet Traffic Transp. **17**, 5 (2005)
4. V. Quaranta, G. D'Altrui, L. Lecce, et al., Beam-forming technique for airplane localization and tracking, in *Paper Presented at Inter-noise, Honolulu, Hawaii, USA*, 3–6 December 2006
5. I.J. Gupta, J.R. Baxter, S.W. Ellingson et al., An experimental study of antenna array calibration. IEEE Trans. Antennas Propag. **51**, 3 (2003)
6. P. Stoica, O. Besson, Computationally efficient maximum likelihood approach to DOA estimation of a scattered source. Wirel. Pers. Commun. **16**, 135–148 (2001)
7. I. Ahmed, W. Perger, Direction finding in the presence of near zone resonant size scattererS. Prog. Electromagn. Res. PIER **5**, 219–234 (2013)
8. T. Aslam, I. Ahmed, M.I. Aslam et al., Direction of arrival estimation in the presence of scatterer in noisy environment. Adv. Electromagn. **6**, 3 (2017)
9. A.M. Elbir, T.E. Tuncer, Far-field DOA estimation and near-field localization for multipath signals. Radio Sci. **49**, 9 (2014)
10. W. Li, X. Mao, Z. Zhai et al., High performance robust adaptive beamforming in the presence of array imperfections. Int. J. Antennas Propag. (2016). https://doi.org/10.1155/2016/3743509
11. H. Ruan, R.C. de Lamare, Robust adaptive beamforming based on low-rank and cross-correlation techniques, in *Paper Presented at 23rd European Signal Processing Conference (EUSIPCO), Nice, France*, 31 August–4 September 2015
12. S. Poormohammad, F. Farzaneh, A. Banai, Direction finding and beamforming using cylindrical array of dipole antennas in the presence of cylindrical scatterer/reflector including the mutual coupling effect. IET Microwaves Antennas Propag. **15**, 5 (2021)
13. M. Al Sharkawy, A.Z. Elsherbeni, S.F. Mahmoud, Electromagnetic scattering from parallel chiral cylinders of circular cross-sections using an iterative procedure. Prog. Electromagn. Res. **47**, 87–110 (2004)
14. C. Balanis (ed.), *Advanced Engineering Electromagnetics*, 2nd edn. (Wiley, New York, 2012)
15. S. Poormohammad, Z. Sasan Nia, F. Farzaneh, DOA error estimation in 3D cylindrical dipole array geometries including the mutual coupling effect. Int. J. Electron. Commun. **84**, 321–330 (2018)
16. N. Ahmadi, S. Poormohammad, F. Farzaneh, Sub-optimal beamforming for 3D cylindrical arrays of dipoles including the mutual coupling effects, in *Paper Presented at 7th Iranian Conference on Electrical Engineering, Yazd, Iran*, 30 April–2 May 2019

Publisher's Note